

**This is the accepted manuscript version of the contribution published as:**

Liu, Y., Fu, J., Wu, L., Kümmel, S., Nijenhuis, I., Richnow, H.H. (2022):  
Characterization of hexachlorocyclohexane isomer dehydrochlorination by LinA1 and LinA2  
using multi-element compound-specific stable isotope analysis  
*Environ. Sci. Technol.* **56** (23), 16848 - 16856 [10.1021/acs.est.2c05334](https://doi.org/10.1021/acs.est.2c05334)

**The publisher's version is available at:**

<http://dx.doi.org/10.1021/acs.est.2c05334>

## 1 Characterization of Hexachlorocyclohexane Isomer 2 Dehydrochlorination by LinA1 and LinA2 Using Multi-element 3 Compound-Specific Stable Isotope Analysis

4 Yaqing Liu, Juan Fu, Langping Wu, Steffen Kümmel, Ivonne Nijenhuis, and Hans H. Richnow\*



Cite This: <https://doi.org/10.1021/acs.est.2c05334>



Read Online

ACCESS |



Metrics & More



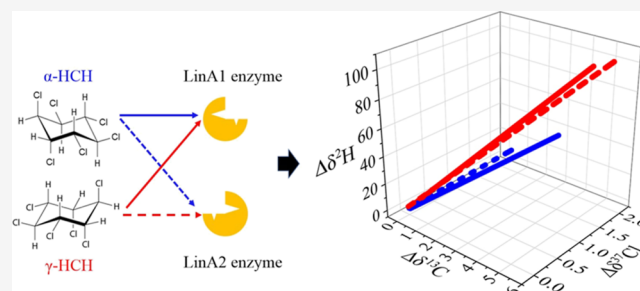
Article Recommendations



Supporting Information

5 **ABSTRACT:** Dehydrochlorination is one of the main (thus far  
6 discovered) processes for aerobic microbial transformation of  
7 hexachlorocyclohexane (HCH) which is mainly catalyzed by LinA  
8 enzymes. In order to gain a better understanding of the reaction  
9 mechanisms, multi-element compound-specific stable isotope  
10 analysis was applied for evaluating  $\alpha$ - and  $\gamma$ -HCH transformations  
11 catalyzed by LinA1 and LinA2 enzymes. The isotopic fractionation  
12 ( $\epsilon_E$ ) values for particular elements of (+)- $\alpha$ -HCH ( $\epsilon_C = -10.7 \pm$   
13  $0.7\%$ ,  $\epsilon_{Cl} = -4.2 \pm 0.5\%$ ,  $\epsilon_H = -154 \pm 16\%$ ) were distinct from  
14 the values for (-)- $\alpha$ -HCH ( $\epsilon_C = -4.1 \pm 0.7\%$ ,  $\epsilon_{Cl} = -1.6 \pm 0.2\%$ ,  
15  $\epsilon_H = -68 \pm 10\%$ ), whereas the dual-isotope fractionation patterns  
16 were almost identical for both enantiomers ( $\Lambda_{C-Cl} = 2.4 \pm 0.4$  and  $2.5 \pm 0.2$ ,  $\Lambda_{H-C} = 12.9 \pm 2.4$  and  $14.9 \pm 1.1$ ). The  $\epsilon_E$  of  $\gamma$ -HCH  
17 transformation by LinA1 and LinA2 were  $-7.8 \pm 1.0\%$  and  $-7.5 \pm 0.8\%$  ( $\epsilon_C$ ),  $-2.7 \pm 0.3\%$  and  $-2.5 \pm 0.4\%$  ( $\epsilon_{Cl}$ ),  $-170 \pm$   
18  $25\%$  and  $-150 \pm 13\%$  ( $\epsilon_H$ ), respectively. Similar  $\Lambda_{C-Cl}$  values ( $2.7 \pm 0.2$  and  $2.9 \pm 0.2$ ) were observed as well as similar  $\Lambda_{H-C}$   
19 values ( $20.1 \pm 2.0$  and  $18.4 \pm 1.9$ ), indicating a similar reaction mechanism by both enzymes during  $\gamma$ -HCH transformation. This is  
20 the first data set on 3D isotope fractionation of  $\alpha$ - and  $\gamma$ -HCH enzymatic dehydrochlorination, which gave a more precise  
21 characterization of the bond cleavages, highlighting the potential of multi-element compound-specific stable isotope analysis to  
22 characterize different transformation processes (e.g., dehydrochlorination and reductive dehalogenation).

23 **KEYWORDS:** transformation, isotope fractionation, pesticides, LinA enzymes, dehydrochlorination



### 24 ■ INTRODUCTION

25 The photocatalytic synthesis of hexachlorocyclohexane  
26 (HCH) yields four main isomers ( $\alpha$ -,  $\beta$ -,  $\gamma$ -, and  $\delta$ -HCH).<sup>1</sup>  
27 Technical HCH (the mixture of different HCH isomers) was  
28 used as a pesticide since the late 1940s until  $\gamma$ -HCH was  
29 identified as the only isomer which possesses insecticidal  
30 activity. Since then,  $\gamma$ -HCH was purified from the other  
31 isomers and marketed as lindane with purities up to 99%.<sup>2-4</sup>  
32 Large amounts of HCH have entered the environment during  
33 agriculture application, and uncontrolled or unconstrained  
34 dumping of waste HCH isomers after lindane was isolated.  
35 Due to their persistence, toxicity, and bioaccumulation, HCH  
36 isomers were added to the list of persistent organic compounds  
37 during the Stockholm Convention in August 2010.<sup>4</sup> However,  
38 many of the stockpiles are still present in contaminated soil  
39 and groundwater and represent a large contaminant reservoir  
40 with about 7 million tons of HCH residuals in the  
41 environment.<sup>5,6</sup>

42 Biotransformation is one of the most promising processes  
43 for the remediation of HCH-contaminated sites. Several  
44 anaerobic cultures have been reported to be able to reduce  
45 HCH by dehalogenation, including *Dehalobacter* and *Dehalo-*  
46 *coccoides*, which can convert HCH by cleaving two C-Cl

bonds.<sup>7-10</sup> In the case of aerobic degradation, more than 30  
47 HCH-degrading *Sphingomonas* have been described and 48  
49 isolated in the last decades.<sup>11-14</sup> Within these cultures, 49  
50 *Sphingobium indicum* B90A, *Sphingobium japonicum* UT26, 50  
51 and *Sphingobium francense* Sp+ have been intensively 51  
52 investigated.<sup>11</sup> Especially, the transformation pathways of 52  
53 HCHs by *S. indicum* B90A and the corresponding enzymes 53  
54 have been studied in detail. Those studies revealed two key 54  
55 enzymes, LinA1 and LinA2, which could catalyze the 55  
56 dehydrochlorination of  $\alpha$ -,  $\gamma$ -, and  $\delta$ -HCH.<sup>15-17</sup> A previous 56  
57 study on the complete genome of strain B90A revealed that it 57  
58 harbors four replicons: one chromosome (3,654,322 bp) and 58  
59 three plasmids designated as pSRL1 (139,218 bp), pSRL2 59  
60 (108,430 bp), and pSRL3 (43,761 bp), where *LinA2* is on the 60  
61 chromosome and *LinA1* is on the pSRL1.<sup>18</sup> Probably due to 61

Received: July 25, 2022

Revised: October 26, 2022

Accepted: October 26, 2022

62 the absence of regulatable promoters and a scattering of the  
63 different genes, both *LinA1* and *LinA2* in strain B90A are  
64 expressed to a constitutive level during the transformation of  $\gamma$ -  
65 HCH.<sup>18</sup> The amino acid sequences of *LinA1* and *LinA2*  
66 enzymes are very similar (90%), differing only by 15 out of 156  
67 amino acids.<sup>19</sup> Remarkably, for  $\alpha$ -HCH, which is the only  
68 HCH isomer possessing two enantiomers, it was demonstrated  
69 that the transformation of (+)- $\alpha$ -HCH is mainly catalyzed by  
70 *LinA1* whereas the (-)- $\alpha$ -HCH transformation is primarily  
71 catalyzed by *LinA2*.<sup>15</sup> The reversal in its preference from the  
72 (-) to the (+)- $\alpha$ -HCH could be the results of the three amino  
73 acid changes in *LinA1*(K20Q, L96C, and A131G) and  
74 enhanced by the change of amino acid T133M.<sup>19,20</sup>  
75 Furthermore, multiple studies have been focused on character-  
76 izing the type of enzymes and their differences which may link  
77 to their catalytic efficiency of the respective ligand by quantum  
78 mechanics/molecular mechanics modeling.<sup>20,21</sup>

79 Bench studies have also been conducted to investigate the  
80 dehydrochlorination mechanisms and reaction pathways.<sup>22,23</sup>  
81 In recent years, compound-specific stable isotope analysis  
82 (CSIA) has been applied for investigating the isotope  
83 fractionation associated with the HCH biotransformation  
84 processes.<sup>16,17,24–27</sup> Isotope fractionation is based on slightly  
85 different reaction kinetics of molecules which differ in their  
86 isotopic composition, as most isotopologues with the light  
87 isotope at the reactive position react faster than isotopologues  
88 possessing the corresponding heavy isotope at the same  
89 position. This normal isotope effect results finally in the  
90 accumulation of the heavier isotopes in the remaining  
91 substrate, whereas the lighter isotopes enrich in the formed  
92 product. The extent of this isotope enrichment can be  
93 quantified by the Rayleigh equation. However, it must be  
94 noted that the observed isotope fractionation can be decreased  
95 due to steps controlling the overall kinetics of the reaction,  
96 prior to the isotope-sensitive bond cleavage. For example, the  
97 binding of the substrate to an enzyme can be a rate-limiting  
98 step of biotransformation reactions and can mask the  
99 biochemical isotope fractionation,<sup>16</sup> which will limit the  
100 application of single element CSIA for investigation of reaction  
101 mechanisms.

102 Methodological advances over the last decade now allow  
103 multi-element compound-specific stable isotope analysis (ME-  
104 CSIA) for overcoming this obstacle, as the masking effect of  
105 isotope enrichment of two elements in one molecule is  
106 expected to be similar.<sup>28,29</sup> Thus, dual-element slopes (e.g., for  
107 carbon and chlorine,  $\Lambda_{C-Cl} = \Delta\delta^{13}C/\Delta\delta^{37}Cl$ , where  $\Delta\delta^{13}C$   
108 and  $\Delta\delta^{37}Cl$  are the changes in isotope compositions of carbon  
109 and chlorine, respectively) can be related to specific reaction  
110 mechanisms. Furthermore, triple-element isotope analysis was  
111 applied for identifying different transformation pathways of  
112 organic compounds, such as herbicide<sup>30</sup> and 1,2-dichloro-  
113 ethane.<sup>31</sup> The  $\Lambda_{C-Cl}$  values for reductive dehalogenation of  
114 HCHs by anaerobic cultures (bond cleavage of two C–Cl  
115 bonds) and the scenarios of bond cleavage have been carefully  
116 discussed in previous studies.<sup>10,32</sup> In the case of aerobic HCH  
117 transformation (dehydrochlorination with the cleavage of C–  
118 H and C–Cl bonds), previous studies only reported the  $\Lambda_{C-H}$   
119 values of HCH,<sup>17,26</sup> which limited the application of ME-CSIA  
120 to distinguish with other reactions (e.g., reductive dehaloge-  
121 nation and anaerobic transformation of HCH with the cleavage  
122 of two C–Cl bonds). Furthermore, in the reactions which  
123 involved two different bond cleavages, for example, C–Cl and

C–H,  $\Lambda_{C-H}$  or  $\Lambda_{C-Cl}$  alone may not be enough for 124  
characterization of the reactions. 125

Therefore, in order to fill the knowledge gaps, the typical 126  
dehydrochlorinases, *LinA1* and *LinA2* enzymes, were used for 127  
 $\alpha$ - and  $\gamma$ -HCH biotransformations. The objectives of this study 128  
were (i) to explore the transformation kinetics of the HCH 129  
isomers by different enzymes, (ii) to determine the isotope 130  
enrichment factors  $\epsilon_C$ ,  $\epsilon_{Cl}$  as well as  $\epsilon_H$  for the HCH isomers, 131  
and (iii) to obtain the  $\Lambda_{C-Cl}$ ,  $\Lambda_{C-H}$  as well as the characteristic 132  
vectors of 3D isotope fractionation during the HCH 133  
biotransformation by dehydrochlorinases. In addition, the 134  
isotopic fractionation patterns obtained in this study were 135  
compared and discussed with the values reported previously 136  
for characterizing different reactions. 137

## 138 ■ EXPERIMENTS AND METHODS

**Experiments.** Enzymatic assays were conducted using 139  
*LinA1* and *LinA2* for the transformation of  $\alpha$ - and  $\gamma$ -HCH, 140  
respectively. The chemicals used in this study are all of 141  
analytical purity grade which are listed in the section of 142  
Chemicals in [Supporting Information](#). The *Escherichia coli* cells 143  
coded with *LinA1* and *LinA2* genes were cultivated for 144  
expression of the *LinA* enzymes. More details of the cultivation 145  
and purification processes can be found in the [Supporting](#) 146  
[Information](#). The enzyme concentrations used in this study 147  
were 75  $\mu\text{g mL}^{-1}$  for *LinA1* and 264  $\mu\text{g mL}^{-1}$  for *LinA2*, 148  
respectively. In contrast to our previous study,<sup>16</sup> both enzymes 149  
were used for the transformation of  $\alpha$ - and  $\gamma$ -HCH. All batch 150  
experiments for HCH transformation were conducted with 151  
Tris buffer (100 mL in 240 mL serum bottle) with an initial 152  
concentration of 5.5  $\mu\text{M}$  of the respective HCH. Reactions 153  
were stopped by adding 0.3% (v/v) formic acid (final 154  
concentration) at different time points resulting in different 155  
extents of HCH transformation. Samples were stored at 4 °C 156  
in the fridge before extraction. The extraction methods are 157  
described in detail in our previous study.<sup>16</sup> More details can be 158  
found in the [Supporting Information](#). 159

**Concentration Analysis.** Concentrations of HCH were 160  
analyzed by GC-FID (Agilent Technologies) and protein 161  
concentrations were analyzed using a NanoDrop ND-1000 162  
spectrophotometer (Thermo Fisher Scientific) as described 163  
previously<sup>16</sup> and summarized in the [Supporting Information](#). 164

**Stable Isotope Analysis.** The carbon isotopic composi- 165  
tions ( $\delta^{13}C$ ) were analyzed by gas chromatography-combus- 166  
tion-isotope ratio mass spectrometry. Analytical details are 167  
described elsewhere for  $\alpha$ -HCH enantiomers<sup>33</sup> and  $\gamma$ -HCH.<sup>10</sup> 168

Hydrogen isotopic compositions ( $\delta^2H$ ) of both HCH 169  
isomers were analyzed by gas chromatography-chromium- 170  
based high-temperature conversion-isotope ratio mass spec- 171  
trometry using the same methods as described by Wu and 172  
colleagues.<sup>34</sup> 173

Chlorine isotopic compositions ( $\delta^{37}Cl$ ) were determined by 174  
gas chromatography-multiple collector-inductively coupled 175  
plasma mass spectrometry, as described elsewhere.<sup>35,36</sup> The 176  
temperature programs and inductively coupled plasma mass 177  
spectrometry parameters were the same as reported in a 178  
previous study.<sup>10</sup> 179

Because the  $\alpha$ -HCH enantiomers could not be measured 180  
separately for  $\delta^{37}Cl$ , the respective  $\delta^{37}Cl$  values were calculated 181  
using eq 1 182

$$\delta_t^{\text{bulk}} = \delta_t^{(-)\alpha\text{-HCH}} \times \text{EF}_t(-) + \delta_t^{(+)\alpha\text{-HCH}} \times \text{EF}_t(+)$$

(1) 183

**Table 1. Summary of Isotopic Fractionation of Different Multi-element Stable Isotope Fractionation Studies Concerning HCH Transformation<sup>a</sup>**

reactions	systems/catalyst	$\alpha$ -HCH					$\gamma$ -HCH					
		$\epsilon_C(\text{‰}) \pm 95\% \text{ CI}$	$\epsilon_{Cl}(\text{‰}) \pm 95\% \text{ CI}$	$\epsilon_H(\text{‰}) \pm 95\% \text{ CI}$	$\Lambda_{C-Cl}$	$\Lambda_{H-C}$	$\epsilon_C(\text{‰}) \pm 95\% \text{ CI}$	$\epsilon_{Cl}(\text{‰}) \pm 95\% \text{ CI}$	$\epsilon_H(\text{‰}) \pm 95\% \text{ CI}$	$\Lambda_{C-Cl}$	$\Lambda_{H-C}$	
dehydrochlorination	LinA1	$-10.8 \pm 1.0^{(+)}$	$-4.2 \pm 0.5^{(+)}$	$-15.4 \pm 16^{(+)}$	$2.4 \pm 0.4^{(+)}$	$12.9 \pm 2.4^{(+)}$	$-7.8 \pm 1.0$	$-2.7 \pm 0.3$	$-170 \pm 25$	$2.7 \pm 0.2$	$20.1 \pm 2.0$	this study
	LinA2	$-4.1 \pm 0.7^{(-)}$	$-1.6 \pm 0.2^{(-)}$	$-68 \pm 10^{(-)}$	$2.5 \pm 0.2^{(-)}$	$14.9 \pm 1.1^{(-)}$	$-7.5 \pm 0.8$	$-2.5 \pm 0.4$	$-150 \pm 13$	$2.9 \pm 0.2$	$18.4 \pm 1.9$	
dehydrochlorination	LinA1	$-3.8 \pm 0.2^{(+)}$					$-8.1 \pm 0.3$		$-122 \pm 6$		$11.5 \pm 0.8$	Liu et al. <sup>16</sup> Schilling et al. <sup>26</sup>
	LinA2						$-8.3 \pm 0.2$		$-160 \pm 6$		$16.4 \pm 0.9$	Schilling et al. <sup>17</sup>
		$-9.6 \pm 0.1^{(+)}/-11.7 \pm 1.5^{(-)}$		$-208 \pm 19^{(+)}$		$22.0 \pm 3.3^{(+)}$						
	LinA variants						$-5.3 \pm 0.8$	$-1.8 \pm 0.4$	$-119 \pm 18$	$2.9 \pm 1.1^*$	$22.5 \pm 6.8^*$	Kannath et al. <sup>27</sup>
	hydrolysis						$-7.0 \pm 0.5$	$-2.0 \pm 0.2$	$-162 \pm 26$	$3.5 \pm 0.6^*$	$23.1 \pm 5.4^*$	
	modeling						$-2.8 \text{ to } -7.5$	$-0.7 \text{ to } -1.5$	$-463 \text{ to } -756$	$3.5 \text{ to } 7.1^*$	$64.1 \text{ to } 263.6^*$	
reductive dehalogenation	<i>Dehalococcoides mccartyi</i> 195	$-3.0 \pm 0.3$	$-1.8 \pm 0.2$		$1.7 \pm 0.2$		$-4.4 \pm 0.6$	$-3.3 \pm 0.4$		$1.2 \pm 0.1$	Liu et al. <sup>10</sup>	
	<i>Dehalococcoides mccartyi</i> BTF08	$-2.4 \pm 0.2$	$-1.4 \pm 0.3$		$1.8 \pm 0.3$		$-4.0 \pm 0.5$	$-3.3 \pm 0.3$		$1.1 \pm 0.3$		
	enrichment culture 1	$-3.0 \pm 0.4$	$-1.4 \pm 0.3$		$2.0 \pm 0.3$		$-4.0 \pm 0.5$	$-2.9 \pm 0.4$		$1.1 \pm 0.2$		
	enrichment culture 2	$-4.2 \pm 0.4$	$-2.0 \pm 0.3$		$1.9 \pm 0.1$		$-3.6 \pm 0.4$	$-3.2 \pm 0.6$		$1.1 \pm 0.1$	Liu et al. <sup>32</sup>	

<sup>a</sup>(+)-values for (+) $\alpha$ -HCH transformation; (-)-values for (-) $\alpha$ -HCH transformation; \*— $\Lambda_{C-Cl}$  values calculated by  $\Lambda_{C-Cl} = \epsilon_C/\epsilon_{Cl}$ .

184 where EF is the enantiomer fraction,  $EF_t(-) = C_t(-)/C_t^{\text{bulk}}$ ,  
185 and  $EF_t(+) = C_t(+)/C_t^{\text{bulk}}$ .

186 For LinA1 experiments, only (+) $\alpha$ -HCH transformation was  
187 observed and thus  $\delta_t^{(-)\alpha\text{-HCH}} = \delta_0^{\text{bulk}}$ ,  $\delta_t^{(+)\alpha\text{-HCH}} = (\delta_t^{\text{bulk}} - EF_t(-)$   
188  $\times \delta_0^{\text{bulk}})/EF_t(+)$ . Similarly for LinA2 experiments, no trans-  
189 formation of (+) $\alpha$ -HCH was observed and thus  $\delta_t^{(+)\alpha\text{-HCH}} =$   
190  $\delta_0^{\text{bulk}}$ ,  $\delta_t^{(-)\alpha\text{-HCH}} = (\delta_t^{\text{bulk}} - EF_t(+)) \times \delta_0^{\text{bulk}}/EF_t(-)$ .

191 **Evaluation of Isotope Data.** The isotopic enrichment  
192 factor of an element E ( $\epsilon_E$ ) was derived using eq 2

$$\ln\left(\frac{\delta^h E_t + 1}{\delta^h E_0 + 1}\right) = \epsilon_E \times \ln\left(\frac{C_t}{C_0}\right) \quad (2)$$

194 where  $\delta^h E_0$  is the initial isotopic signature of the substrate,  $\delta^h E_t$   
195 is the isotopic composition of the substrate at time  $t$ , and  $C_t/C_0$   
196 is the fraction of the remaining substrate.

197 For the determination of lambda values ( $\Lambda$ ), hydrogen  
198 versus carbon isotope discrimination ( $\Lambda_{H-C} = \Delta\delta^2\text{H}/\Delta\delta^{13}\text{C}$ )  
199 and carbon versus chlorine isotope discrimination ( $\Lambda_{C-Cl} =$   
200  $\Delta\delta^{13}\text{C}/\Delta\delta^{37}\text{Cl}$ ) were plotted and the respective  $\Lambda$  was derived  
201 from the slope of the linear regression. The uncertainty of  $\Lambda$ ,  
202 given as the 95% confidence interval (CI), was derived from  
203 regression analysis using Origin 9.0.

204 The triple-element isotope plotting was also done using  
205 Origin 9.0 and the characteristic unit vectors were determined  
206 following the approach of Palau et al.<sup>31</sup> To further assess the  
207 similarities and differences between the unit vectors, the angle  
208  $\theta$  between the two vectors were calculated following the  
209 method described by Palau et al.<sup>31</sup>

## RESULTS AND DISCUSSION

210

**Transformation of  $\alpha$ - and  $\gamma$ -HCH Catalyzed by LinA Enzymes.**  *$\alpha$ -HCH.* In the LinA1 experiment (reaction time, 2  
211 h), only (+) $\alpha$ -HCH transformation was observed with a  
212 reaction rate of  $0.2 \pm 0.01 \text{ h}^{-1}$  (Supporting Information, Figure  
213 1) and pentachlorocyclohexane (PCCH) was the major  
214 product. Similarly, only (-) $\alpha$ -HCH transformation was  
215 observed in the LinA2 experiment (reaction time, 1.5 h)  
216 with a reaction rate of  $0.4 \pm 0.03 \text{ h}^{-1}$  (Supporting Information,  
217 Figure 1) and PCCH was the main product. The trans-  
218 formation products indicated that a dehydrochlorination  
219 reaction similar to chemical hydrolysis took place. LinA1 and  
220 LinA2 showed a selective transformation of (+) and (-) $\alpha$ -  
221 HCH, respectively, which was the same as we observed  
222 before.<sup>16</sup> In contrast, a previous study reported that both  
223 enantiomers could be degraded by LinA1 or LinA2 if the  
224 reaction lasted for 24 h.<sup>15</sup> However, the transformation rate for  
225 (+) $\alpha$ -HCH ( $0.43 \pm 0.03 \text{ h}^{-1}$ ) was much higher than that for  
226 (-) $\alpha$ -HCH ( $0.060 \pm 0.010 \text{ h}^{-1}$ ) when LinA1 was used for the  
227 catalysis. Similarly, when LinA2 was used, a higher trans-  
228 formation rate for (-) $\alpha$ -HCH ( $0.47 \pm 0.06 \text{ h}^{-1}$ ) than that for  
229 (+) $\alpha$ -HCH ( $0.04 \pm 0.006 \text{ h}^{-1}$ ) was observed. The difference  
230 in the selectivity is probably due to the smaller amounts of  
231 enzymes which we have applied in our study. Similar results  
232 have been reported for experiments with relatively low  
233 concentrations of LinA2 ( $0.01 \mu\text{g mL}^{-1}$ ), where only (-) $\alpha$ -  
234 HCH transformation was observed.<sup>17</sup> Yet, when the  
235 concentration of LinA2 was increased ( $0.7 \mu\text{g mL}^{-1}$ ), both  
236 (+) and (-) $\alpha$ -HCH were degraded.<sup>17</sup> Accordingly, the  
237  
238

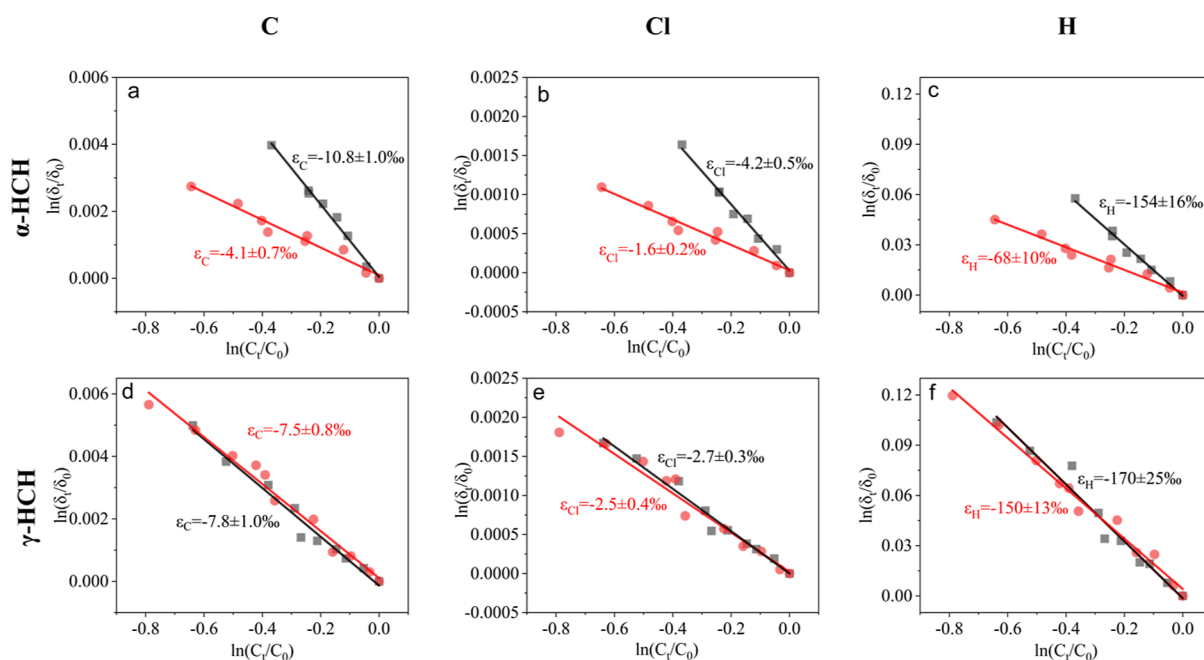


**Figure 1.** Rayleigh plots for carbon, chlorine, and hydrogen isotopic fractionation during the transformation of  $\alpha$ -HCH (a–c) and  $\gamma$ -HCH (d–f) by LinA1 (black symbols) and LinA2 (red symbols). Note, graphs for transformation experiments with LinA1 include only data of (+) $\alpha$ -HCH, whereas LinA2 experiments include only data of (–) $\alpha$ -HCH because in those experiments only one of the two enantiomers was transformed by the respective enzyme.

239 enzyme amount may affect the transformation of the different  
240 enantiomers. The enantiomer fractionation, which is a result of  
241 different transformation rates of the enantiomers, could be  
242 variable as binding to the enzyme could take place even when  
243 it is stereochemically unfavorable. Thus, the variability of  
244 enantiomer fractionation will limit its application for evaluating  
245 biotic transformation processes as the relatively high enzyme-  
246 to-substrate ratio may decrease specific binding to the  
247 enzymes.

248  $\gamma$ -HCH. Both LinA1 and LinA2 showed comparable  
249 transformation rates of  $0.3 \pm 0.01 \text{ h}^{-1}$  (LinA1) and  $0.3 \pm$   
250  $0.02 \text{ h}^{-1}$  (LinA2) for  $\gamma$ -HCH (Supporting Information, Figure  
251 1), and the major product identified was also PCCH. This is in  
252 agreement with a previous study which demonstrated that  $\gamma$ -  
253 HCH could be degraded by both LinA1 and LinA2 enzymes.<sup>26</sup>  
254 In our study, both enzymes showed relatively fast trans-  
255 formation rates for  $\gamma$ -HCH compared to that for bulk  $\alpha$ -HCH  
256 ( $0.063 \pm 0.016$  and  $0.19 \pm 0.059 \text{ h}^{-1}$  in the experiments with  
257 LinA1 and LinA2, respectively), which supports the  
258 speculation of a previous study that  $\gamma$ -HCH transformation is  
259 easier in comparison to  $\alpha$ -HCH transformation, as  $\gamma$ -HCH  
260 possesses one more C–Cl bond in the axial position (as shown  
261 in Figure SI3, Supporting Information), which is most likely  
262 the preferred position for bond cleavages.<sup>37</sup>

263 **Isotopic Fractionation of  $\alpha$ - and  $\gamma$ -HCH Catalyzed by**  
264 **LinA Enzymes.**  $\alpha$ -HCH. Significant normal carbon, chlorine,  
265 and hydrogen isotopic fractionation were observed during the  
266 transformation of  $\alpha$ -HCH enantiomers by LinA1 and LinA2 as  
267 shown in Supporting Information, Figure 2. In the case of  
268 (+) $\alpha$ -HCH transformation (catalyzed by LinA1), the isotopic  
269 fractionation of carbon ( $\epsilon_{C-(+)\alpha\text{-HCH}}$ ), chlorine ( $\epsilon_{Cl-(+)\alpha\text{-HCH}}$ ),  
270 and hydrogen ( $\epsilon_{H-(+)\alpha\text{-HCH}}$ ) were  $-10.8 \pm 1.0$ ,  $-4.2 \pm 0.5$ , and  
271  $-154 \pm 16\%$ , respectively (Table 1, Figure 1). In contrast, the  
272 isotopic fractionation of (–) $\alpha$ -HCH (catalyzed by LinA2) was

comparatively low ( $\epsilon_{C-(-)\alpha\text{-HCH}} = -4.1 \pm 0.7\%$ ,  $\epsilon_{Cl-(-)\alpha\text{-HCH}} = 273$   
 $-1.6 \pm 0.2\%$ ,  $\epsilon_{H-(-)\alpha\text{-HCH}} = -68 \pm 10\%$ , Table 1, Figure 1). 274

The obtained  $\epsilon_{C-(+)\alpha\text{-HCH}}$  ( $-10.8 \pm 1.0\%$ ) catalyzed by 275  
LinA1 was similar to the value previously reported ( $-9.6 \pm 276$   
 $0.1\%$ ) for the transformation of (+) $\alpha$ -HCH by LinA2<sup>17</sup> and 277  
to the values (average =  $-11.1 \pm 0.3\%$ ) reported for the 278  
transformation of (+) $\alpha$ -HCH by LinA1.<sup>16</sup> In contrast, the 279  
 $\epsilon_{H-(+)\alpha\text{-HCH}}$  determined in the present study ( $-154 \pm 16\%$ ) 280  
was lower than the value ( $-208 \pm 19\%$ ) reported for the 281  
transformation of (+) $\alpha$ -HCH by LinA2.<sup>17</sup> The  $\epsilon_{C-(-)\alpha\text{-HCH}}$  282  
value ( $-4.1 \pm 0.7\%$ ) catalyzed by LinA2 was almost identical 283  
to the values (average =  $-3.8 \pm 0.2\%$ ) reported previously.<sup>16</sup> 284  
The observed differences in the  $\epsilon$  values for the transformation 285  
of  $\alpha$ -HCH by LinA1 and LinA2 enzymes could result from the 286  
different kinetic isotope effects. However, it is more likely that 287  
those differences were the result of masking effects of the 288  
isotope fractionation caused by steps prior to the bond 289  
cleavage reaction (e.g., commitment to catalysis) which is 290  
further supported by the findings of a study reporting a higher 291  
 $\epsilon_{C-(-)\alpha\text{-HCH}}$  value ( $-11.7 \pm 1.5\%$ ) for the transformation of 292  
(–) $\alpha$ -HCH by LinA2.<sup>17</sup> Accordingly, the occurrence of 293  
masking effects may also explain that when the concentration 294  
of LinA2 was much higher (which resulted in a too fast 295  
reaction), no isotope fractionation of (–) $\alpha$ -HCH can be 296  
detected as described previously.<sup>17</sup> However, it should be 297  
noted that the higher  $\epsilon_{C-(-)\alpha\text{-HCH}}$  value of  $-11.7 \pm 1.5\%$  was 298  
only approximated from the isotope signatures of the substrate 299  
and the dechlorinated product, whereas hydrogen isotope 300  
fractionation was not determined.<sup>17</sup> It is plausible that the 301  
variability of hydrogen isotope fractionation is much higher. 302

Furthermore, previous studies reported carbon and chlorine 303  
isotopic fractionation of bulk  $\alpha$ -HCH during anaerobic 304  
transformation ranging from  $-2.4 \pm 0.2$  to  $-4.2 \pm 0.4\%$  for 305  
 $\epsilon_{C-\alpha\text{-HCH}}$  and from  $-1.4 \pm 0.3$  to  $-2.0 \pm 0.3\%$  for  $\epsilon_{Cl-\alpha\text{-HCH}}$  306  
respectively.<sup>10,32</sup> As no enantiomer fractionation during 307

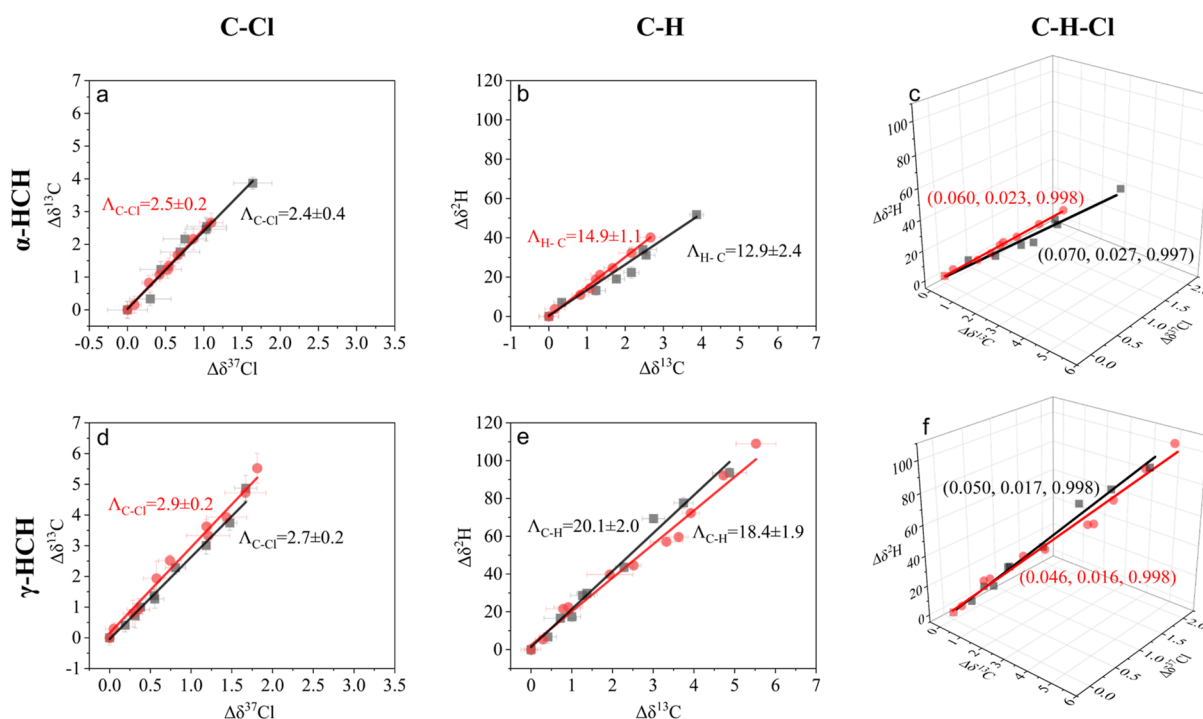


**Figure 2.** ME-isotopic fractionation plots for the determination of  $\Lambda_{\text{C-Cl}}$  and  $\Lambda_{\text{H-C}}$  and 3D plotting during the transformation of  $\alpha$ -HCH (a–c) and  $\gamma$ -HCH (d–f) by LinA1 (black) and LinA2 (red). Note, graphs for transformation experiments with LinA1 include only data of (+) $\alpha$ -HCH, whereas LinA2 experiments include only data of (–) $\alpha$ -HCH because in those experiments only one of the two enantiomers was transformed by the respective enzyme.

308 anaerobic  $\alpha$ -HCH transformation was observed and the  
 309 detected  $\epsilon_{\text{C}}$  of (+)- and (–) $\alpha$ -HCH were identical, it indicates  
 310 that the values of  $\epsilon_{\text{Cl}}$  for both enantiomers were also the  
 311 same.<sup>10</sup> As mentioned above, anaerobic  $\alpha$ -HCH trans-  
 312 formation is a reductive dehalogenation process,<sup>10</sup> whereas  
 313 LinA enzymes catalyze a dehydrochlorination reaction.<sup>26</sup>  
 314 Therefore, the general expectation is that both processes  
 315 would result in different isotope fractionation patterns.<sup>38</sup> The  
 316 aerobic (dehydrochlorination) and the anaerobic (–) $\alpha$ -HCH  
 317 transformation (reductive dehalogenation) resulted in a  
 318 comparable carbon and chlorine isotopic fractionation, which  
 319 was not the case for (+) $\alpha$ -HCH. Further studies on hydrogen  
 320 isotope fractionation may give a better characterization of the  
 321 different reactions.

322  $\gamma$ -HCH. The transformation of  $\gamma$ -HCH by LinA1 and LinA2  
 323 resulted in a comparable isotopic fractionation for carbon  
 324 ( $\epsilon_{\text{C-}\gamma\text{-HCH}} = -7.8 \pm 1.0$  and  $-7.5 \pm 0.8\text{‰}$ ), chlorine ( $\epsilon_{\text{Cl-}\gamma\text{-HCH}}$   
 325  $= -2.7 \pm 0.3$  and  $-2.5 \pm 0.4\text{‰}$ ), and hydrogen ( $\epsilon_{\text{H-}\gamma\text{-HCH}} =$   
 326  $-170 \pm 25$  and  $-150 \pm 13\text{‰}$ ). These isotopic fractionations  
 327 were consistent with the values reported for the hydrolysis of  $\gamma$ -  
 328 HCH ( $\epsilon_{\text{C-}\gamma\text{-HCH}} = -7.0 \pm 0.5\text{‰}$ ,  $\epsilon_{\text{Cl-}\gamma\text{-HCH}} = -2.0 \pm 0.2\text{‰}$ , and  
 329  $\epsilon_{\text{H-}\gamma\text{-HCH}} = -162 \pm 26\text{‰}$ ).<sup>27</sup> Moreover, the isotopic  
 330 fractionations determined in the present study were also in  
 331 agreement with  $\epsilon_{\text{C-}\gamma\text{-HCH}}$  and  $\epsilon_{\text{H-}\gamma\text{-HCH}}$  ( $-8.3 \pm 0.2$  and  $160 \pm$   
 332  $6\text{‰}$ ) reported for  $\gamma$ -HCH transformation by LinA2.<sup>26</sup> In  
 333 addition,  $\gamma$ -HCH transformation by LinA1 resulted in an  
 334 increased  $\epsilon_{\text{H-}\gamma\text{-HCH}}$  in comparison to the previously reported  
 335 value ( $\epsilon_{\text{H-}\gamma\text{-HCH}} = -122 \pm 6\text{‰}$ ), whereas  $\epsilon_{\text{C-}\gamma\text{-HCH}}$  was almost  
 336 identical ( $\epsilon_{\text{C-}\gamma\text{-HCH}} = -8.1 \pm 0.3\text{‰}$ ; Table 1). The relatively  
 337 high variability of the hydrogen isotopic fractionation observed  
 338 for  $\gamma$ -HCH transformation agrees with the results obtained for  
 339  $\alpha$ -HCH transformation in the present study. However, in  
 340 comparison to the values of another LinA variant, which were

– $5.3 \pm 0.8\text{‰}$  for  $\epsilon_{\text{C-}\gamma\text{-HCH}}$ ,  $-1.8 \pm 0.4\text{‰}$  for  $\epsilon_{\text{Cl-}\gamma\text{-HCH}}$ , and  $341$   
 $-119 \pm 18\text{‰}$  for  $\epsilon_{\text{H-}\gamma\text{-HCH}}$ ,<sup>27</sup> the values determined in the  $342$   
 present study were higher. This difference could be a result of  $343$   
 masking effects or it could be caused by slightly different  $344$   
 reaction mechanisms of the LinA variants leading to different  $345$   
 isotope fractionation patterns. Compared with the reductive  $346$   
 dehalogenation of  $\gamma$ -HCH (Table 1),  $\epsilon_{\text{C-}\gamma\text{-HCH}}$  and  $\epsilon_{\text{Cl-}\gamma\text{-HCH}}$   $347$   
 obtained were higher in the present study. In addition, the  $\epsilon$   $348$   
 values obtained from modeling studies showed much lower  $349$   
 values compared with the experiment data, except  $\epsilon_{\text{H}}$ .  $350$

**ME-Isotopic Analysis of  $\alpha$ - and  $\gamma$ -HCH Dehydrochlorination Catalyzed by LinA Enzymes.**  $\alpha$ -HCH. The isotopic  $351$   
 fractionation of  $\alpha$ -HCH enantiomer dehydrochlorination were  $352$   
 correlated by dual-element isotope analyses and the corre-  $353$   
 sponding  $\Lambda_{\text{C-Cl}}$  and  $\Lambda_{\text{H-C}}$  values, expressing the mode of the  $354$   
 C–Cl and C–H bond cleavage mechanisms, were calculated  $355$   
 (Table 1, Figure 2a,b). The almost identical  $\Lambda$  values for both  $356$   
 enantiomers indicate that the reaction mechanism of LinA1  $357$   
 transforming (+) $\alpha$ -HCH and LinA2 converting (–) $\alpha$ -HCH is  $358$   
 quite similar. So far, there is only one  $\Lambda_{\text{H-C}}$  value available in  $359$   
 the literature which is based on the transformation of (+) $\alpha$ -  $360$   
 HCH by LinA2.<sup>17</sup> In comparison to this  $\Lambda_{\text{H-C}}$  value ( $22.0 \pm$   $361$   
 $3.3$ ), the  $\Lambda_{\text{H-C}}$  value of (+) $\alpha$ -HCH transformation by LinA1  $362$   
 ( $12.9 \pm 2.4$ ) determined in the present study is significantly  $363$   
 lower. As dual-element isotope analysis can theoretically omit  $364$   
 masking of isotope effects, this difference indicates different  $365$   
 commitments to catalysis, for example, the specific mode of  $366$   
 binding in the enzyme pocket prior to catalysis. This could be a  $367$   
 result of the three amino acid changes in LinA1, that is, K20Q,  $368$   
 L96C, and A131G,<sup>19,20</sup> which caused a reversal in its  $369$   
 preference from the conversion of (–) to (+) $\alpha$ -HCH.  $370$   
 Furthermore, as the amino acid change T133M enhanced  $371$   
 the enantiomer preference,<sup>19,20</sup> this could be also the  $372$   
 $373$

374 additional reasons for the different isotope fractionation  
375 patterns. In addition, previous studies reported that LinA1  
376 and LinA2 differ in the rate of (+) $\alpha$ -HCH transformation,<sup>15,17</sup>  
377 which could be an indicator for different commitments to  
378 catalysis as well. Furthermore, compared to the  $\Lambda_{C-Cl}$  values  
379 obtained from the  $\alpha$ -HCH anaerobic transformation (ranging  
380 from  $1.7 \pm 0.2$  to  $2.0 \pm 0.3$ ),<sup>10</sup> the  $\Lambda_{C-Cl}$  values of the aerobic  
381 transformation ( $2.4 \pm 0.4$  for (+) $\alpha$ -HCH transformation by  
382 LinA1 and  $2.5 \pm 0.2$  for (-) $\alpha$ -HCH transformation by LinA2)  
383 show a trend to larger but still overlapping values and thus do  
384 not allow distinguishing between aerobic and anaerobic  $\alpha$ -  
385 HCH transformation at field sites.

386 The C, H, and Cl isotope data for the dehydrochlorination  
387 of  $\alpha$ -HCH enantiomers were also combined in a 3D isotope  
388 plot. Characteristic unit vectors were determined as (0.070,  
389 0.027, 0.997) and (0.060, 0.023, 0.998) for (-) and (+) $\alpha$ -  
390 HCH (Figure 2c), respectively. The calculated angle  $\theta$   
391 between the two vectors is less than  $1^\circ$ . The vectors as well  
392 as the plots show clearly same trends for the transformation of  
393 (-) and (+) $\alpha$ -HCH by LinA1 and LinA2, respectively. This  
394 result indicates that the dehydrochlorination can be well  
395 characterized by triple-element isotope analysis. Furthermore,  
396 this triple-element isotope analysis would give a chance to  
397 distinguish different HCH transformation pathways, for  
398 example, dehydrochlorination and reductive dehalogenation.  
399 As dehydrochlorination involves both C-Cl and C-H bond  
400 cleavage whereas reductive dehalogenation only involves C-Cl  
401 bond cleavage and no significant hydrogen isotope fractiona-  
402 tion is expected, secondary hydrogen isotope fractionation may  
403 occur. In the future, hydrogen isotope fractionation may add as  
404 a further criterion to identify processes, but hydrogen isotopic  
405 fractionation values for HCH reductive dehalogenation are not  
406 yet available to our best knowledge.

407  $\gamma$ -HCH. The  $\Lambda_{C-Cl}$  and  $\Lambda_{H-C}$  values for the aerobic  
408 transformation of  $\gamma$ -HCH catalyzed by LinA1 and LinA2  
409 were almost identical (Table 1, Figure 2d,e), which indicates  
410 that the dehydrochlorination mechanisms catalyzed by LinA1  
411 and LinA2 lead to the same isotope effects. It is plausible that  
412 the different amino acids in LinA1 and LinA2 enzymes did not  
413 cause any different commitments to catalysis and led to the  
414 same isotope fractionation patterns. This is also in agreement  
415 with previous studies that 4 out of the 10 amino acids vicinal to  
416 the active site of LinA might govern the enantioselectivity  
417 toward  $\alpha$ -HCH enantiomers, but do not necessarily play a  
418 similar role in the transformation of  $\gamma$ -HCH.<sup>19,20</sup> Based on the  
419 reported  $\epsilon_C$  and  $\epsilon_{Cl}$ ,<sup>27</sup> the  $\Lambda_{C-Cl}$  values of  $\gamma$ -HCH for the  
420 chemical hydrolysis and the enzymatic catalysis by LinA  
421 variants were calculated to be  $3.5 \pm 0.6$  and  $2.9 \pm 1.1$ ,  
422 respectively (Table 1). The  $\Lambda_{C-Cl}$  values for  $\gamma$ -HCH  
423 transformation by LinA variants based on Kannath's study  
424 ( $2.9 \pm 1.1$ ) and the respective  $\Lambda_{C-Cl}$  values determined in the  
425 present study ( $2.7 \pm 0.2$  by LinA1 and  $2.9 \pm 0.2$  by LinA2) are  
426 not distinguishable, indicating similar reaction mechanisms.  
427 The  $\Lambda_{C-Cl}$  value ( $3.5 \pm 0.6$ ) of  $\gamma$ -HCH during chemical  
428 hydrolysis showed some differences to the values obtained  
429 during dehydrochlorination but still overlapping, which  
430 indicates the uncertainty for characterizing the bond cleavage  
431 (C-Cl and C-H) by dual-isotope analysis.

432 Furthermore, the  $\Lambda_{C-Cl}$  values for  $\gamma$ -HCH dehydrochlori-  
433 nation ( $>2.7 \pm 0.2$ ) can be distinguished from the  $\Lambda_{C-Cl}$  values  
434 that have been reported for  $\gamma$ -HCH reductive dehalogenation  
435 ( $<1.2 \pm 0.1$ ),<sup>10</sup> thus enabling the differentiation of  
436 dehydrochlorination from reductive dehalogenation by dual-

element isotope analysis. It should be noted that the  $\Lambda_{H-C}$   
values reported in Schilling et al. (2019b) for  $\gamma$ -HCH  
transformation by LinA1 and LinA2 were lower than those  
determined in the present study (Table 1), which is most likely  
caused by the higher variability of hydrogen isotope  
fractionation. Furthermore, the  $\Lambda_{C-Cl}$  and  $\Lambda_{H-C}$  values from  
modeling (Table 1) also show significant differences compared  
with the experimental data, which indicates that the actual  
reactions are much more complex than the simulated models.  
Furthermore, it is plausible that  $\Lambda_{H-C}$  values possess a  
relatively high variability compared to the  $\Lambda_{C-Cl}$  values,  
which is in comparison to other elements (e.g., C and Cl)  
most likely due to the more pronounced sensitivity of the  
hydrogen isotope fractionation and due to the existence of  
relatively strong secondary isotope effects.

Similar as  $\alpha$ -HCH, the triple-element isotope fractionation  
of  $\gamma$ -HCH transformed by LinA1 and LinA2 were plotted as  
shown in Figure 2f. The characteristic unit vectors were (0.050,  
0.017, 0.999) and (0.046, 0.016, 0.999) for the transformation  
by LinA1 and LinA2, respectively. The characteristic unit  
vectors of  $\gamma$ -HCH transformation by LinA variants and  
chemical hydrolysis in a previous study<sup>27</sup> were calculated as  
(0.044, 0.015, 0.999) and (0.043, 0.012, 0.999), which were  
almost identical to our results. Also, the angle  $\theta$  between these  
four vectors are all less than  $1^\circ$ . Compared to the character-  
ization of bond cleavages (C-Cl and C-H) by  $\Lambda_{C-Cl}$  value  
which showed difference to some extent as we discussed, the  
triple-element isotope analysis will give a more precise  
evaluation. As already discussed for  $\alpha$ -HCH transformation,  
the triple-element isotopic fractionation analysis will give a  
great chance for distinguishing different transformation  
pathways of HCHs, for example, dehydrochlorination and  
reductive dehalogenation, at field sites.

**Environmental Significance.** Enantiomer fractionation  
was applied in many studies for quantification of biotransfor-  
mation of organic compounds in the environment. Together  
with previous studies, we confirmed that the selectivity of  $\alpha$ -  
HCH enantiomers by LinA enzymes can be lowered when the  
enzyme concentration was relatively high, which indicates that  
the application of enantiomer fractionation for quantification  
of biotic transformation may lead to bias to some extent.

In our study, the extent of isotope fractionation indicates  
primary  $^2H$ ,  $^{13}C$ , and  $^{37}Cl$  isotope effects in the rate-limiting  
bond cleavage steps, the dual- as well as triple-element isotope  
analyses show similar isotope fractionation trends for both  $\alpha$ -  
and  $\gamma$ -HCH during the transformation by LinA1 and LinA2.  
The experimental data from biotransformation of  $\gamma$ -HCH  
compared with molecular modeling in a previous report<sup>27</sup>  
show remarkable differences indicating that the application of  
molecular modeling for field site evaluation needs improve-  
ments.

In addition to elucidating natural biodegradation processes  
for HCHs, ME-CSIA can also be useful for obtaining insights  
into degradation processes, for example, both aerobic and  
anaerobic transformations may happen with the changing of  
geochemistry. Furthermore, the new isotope fractionation  
values for  $\alpha$ - and  $\gamma$ -HCH determined in this study, with both  
LinA1 and LinA2 enzymes, open opportunities for using triple-  
element CSIA to identify HCH transformation processes in  
different environmental compartments, such as soil, sediments  
trees, wheat, and even in mammals.

## 498 ■ ASSOCIATED CONTENT

## 499 ■ Supporting Information

500 The Supporting Information is available free of charge at  
501 <https://pubs.acs.org/doi/10.1021/acs.est.2c05334>.

502 Additional experimental details, materials, and methods;  
503 data on the degradation kinetics and multi-element  
504 isotope fractionation of  $\alpha$ -HCH degradation experi-  
505 ments; and chemical structure of (+)/(-) $\alpha$ -HCH and  $\gamma$ -  
506 HCH (PDF)

## 507 ■ AUTHOR INFORMATION

## 508 Corresponding Author

509 Hans H. Richnow – Department of Isotope Biogeochemistry,  
510 Helmholtz Centre for Environmental Research-UFZ, Leipzig  
511 04318, Germany; Isodetect, Leipzig 04103, Germany;  
512 [orcid.org/0000-0002-6144-4129](https://orcid.org/0000-0002-6144-4129);  
513 Email: [hans.richnow@ufz.de](mailto:hans.richnow@ufz.de)

## 514 Authors

515 Yaqing Liu – College of Light Industry and Food Engineering,  
516 Guangxi Key Laboratory of Clean Pulp & Papermaking and  
517 Pollution Control, Guangxi University, Nanning 530004,  
518 P.R. China; [orcid.org/0000-0003-2841-9551](https://orcid.org/0000-0003-2841-9551)

519 Juan Fu – College of Light Industry and Food Engineering,  
520 Guangxi Key Laboratory of Clean Pulp & Papermaking and  
521 Pollution Control, Guangxi University, Nanning 530004,  
522 P.R. China; [orcid.org/0000-0002-5478-6075](https://orcid.org/0000-0002-5478-6075)

523 Langping Wu – Department of Isotope Biogeochemistry,  
524 Helmholtz Centre for Environmental Research-UFZ, Leipzig  
525 04318, Germany; Ecometrix Incorporated, Mississauga,  
526 Ontario L5N 2L8, Canada; [orcid.org/0000-0003-0599-7172](https://orcid.org/0000-0003-0599-7172)

528 Steffen Kümmel – Department of Isotope Biogeochemistry,  
529 Helmholtz Centre for Environmental Research-UFZ, Leipzig  
530 04318, Germany; [orcid.org/0000-0002-8114-8116](https://orcid.org/0000-0002-8114-8116)

531 Ivonne Nijenhuis – Department of Isotope Biogeochemistry,  
532 Helmholtz Centre for Environmental Research-UFZ, Leipzig  
533 04318, Germany; [orcid.org/0000-0001-9737-9501](https://orcid.org/0000-0001-9737-9501)

534 Complete contact information is available at:

535 <https://pubs.acs.org/10.1021/acs.est.2c05334>

## 536 Notes

537 The authors declare no competing financial interest.

## 538 ■ ACKNOWLEDGMENTS

539 The authors would like to thank Prof. Rup Lal from the  
540 Molecular Biology Laboratory, the University of Delhi, India,  
541 for providing the clone *E. coli* BL21 (AI) containing LinA1 and  
542 LinA2. Moreover, the authors are thankful for using the  
543 analytical facilities of the Centre for Chemical Microscopy  
544 (ProVIS) at UFZ Leipzig, which is supported by the European  
545 Regional Development Funds (EFRE-Europe funds Saxony)  
546 and the Helmholtz Association. This research was supported  
547 by the Guangxi Natural Science Foundation  
548 (2021GXNSFBA196092 and AD22080067) and the Opening  
549 Project of Guangxi Key Laboratory of Clean Pulp &  
550 Papermaking and Pollution Control (2021KF40).

## 551 ■ REFERENCES

552 (1) Sang, S.; Petrovic, S.; Cuddeford, V., *Lindane—a Review of*  
553 *Toxicity and Environmental Fate*; World Wildl Fund Can, 1999; p  
554 1724.

(2) Slade, R. E. The gamma-isomer of hexachlorocyclohexane. *Chem. Ind.* **1945**, 65, 314–319. 555

(3) Nagata, Y.; Endo, R.; Ito, M.; Ohtsubo, Y.; Tsuda, M. Aerobic degradation of lindane ( $\gamma$ -hexachlorocyclohexane) in bacteria and its biochemical and molecular basis. *Appl. Microbiol. Biotechnol.* **2007**, 76, 559–560. 557

(4) Vijgen, J.; Abhilash, P.; Li, Y. F.; Lal, R.; Forter, M.; Torres, J.; Singh, N.; Yunus, M.; Tian, C.; Schäffer, A.; Weber, R. Hexachlorocyclohexane (HCH) as new Stockholm Convention POPs—a global perspective on the management of Lindane and its waste isomers. *Environ. Sci. Pollut. Res.* **2011**, 18, 152–162. 561

(5) Vijgen, J.; de Borst, B.; Weber, R.; Stobiecki, T.; Forter, M. HCH and lindane contaminated sites: European and global need for a permanent solution for a long-time neglected issue. *Environ. Pollut.* **2019**, 248, 696–705. 562

(6) Tripathi, V.; Edrisi, S. A.; Chaurasia, R.; Pandey, K. K.; Dinesh, D.; Srivastava, R.; Srivastava, P.; Abhilash, P. C. Restoring HCHs polluted land as one of the priority activities during the UN-International Decade on Ecosystem Restoration (2021–2030): A call for global action. *Sci. Total Environ.* **2019**, 689, 1304–1315. 563

(7) Doesburg, W.; Eekert, M. H. A.; Middeldorp, P. J. M.; Balk, M.; Schraa, G.; Stams, A. J. M. Reductive dechlorination of beta-hexachlorocyclohexane (beta-HCH) by a *Dehalobacter* species in coculture with a *Sedimentibacter* sp. *FEMS Microbiol. Ecol.* **2005**, 54, 87–95. 564

(8) Kaufhold, T.; Schmidt, M.; Cichocka, D.; Nikolausz, M.; Nijenhuis, I. Dehalogenation of diverse halogenated substrates by a highly enriched *Dehalococcoides*-containing culture derived from the contaminated mega-site in Bitterfeld. *FEMS Microbiol. Ecol.* **2013**, 83, 176–188. 565

(9) Bashir, S.; Kuntze, K.; Vogt, C.; Nijenhuis, I. Anaerobic biotransformation of hexachlorocyclohexane isomers by *Dehalococcoides* species and an enrichment culture. *Biodegradation* **2018**, 29, 409–418. 566

(10) Liu, Y.; Liu, J.; Renpenning, J.; Nijenhuis, I.; Richnow, H.-H. Dual C–Cl Isotope Analysis for Characterizing the Reductive Dechlorination of  $\alpha$ - and  $\gamma$ -Hexachlorocyclohexane by Two *Dehalococcoides mccartyi* Strains and an Enrichment Culture. *Environ. Sci. Technol.* **2020**, 54, 7250–7260. 567

(11) Lal, R.; Pandey, G.; Sharma, P.; Kumari, K.; Malhotra, S.; Pandey, R.; Raina, V.; Kohler, H. P.; Holliger, C.; Jackson, C.; Oakeshott, J. G. Biochemistry of microbial degradation of hexachlorocyclohexane and prospects for bioremediation. *Microbiol. Mol. Biol. Rev.* **2010**, 74, 58–80. 568

(12) Manickam, N.; Bajaj, A.; Saini, H. S.; Shanker, R. Surfactant mediated enhanced biodegradation of hexachlorocyclohexane (HCH) isomers by *Sphingomonas* sp. NM05. *Biodegradation* **2012**, 23, 673–682. 569

(13) Tabata, M.; Ohtsubo, Y.; Ohhata, S.; Tsuda, M.; Nagata, Y. Complete Genome Sequence of the  $\gamma$ -Hexachlorocyclohexane-Degrading Bacterium *Sphingomonas* sp. Strain MM-1. *Genome Announc.* **2013**, 1, No. e00247. 570

(14) Alvarez, A.; Rodríguez-Garrido, B.; Cerdeira-Pérez, A.; Tomás-Pérez, A.; Kidd, P.; Prieto-Fernández, A. Enhanced biodegradation of hexachlorocyclohexane (HCH) isomers by *Sphingobium* sp. strain D4 in the presence of root exudates or in co-culture with HCH-mobilizing strains. *J. Hazard. Mater.* **2022**, 433, 128764. 571

(15) Suar, M.; Hauser, A.; Poiger, T.; Buser, H. R.; Müller, M. D.; Dogra, C.; Raina, V.; Holliger, C.; van der Meer, J. R.; Lal, R.; Kohler, H. P. Enantioselective transformation of alpha-hexachlorocyclohexane by the dehydrochlorinases LinA1 and LinA2 from the soil bacterium *Sphingomonas paucimobilis* B90A. *Appl. Environ. Microbiol.* **2005**, 71, 8514–8518. 572

(16) Liu, Y.; Wu, L.; Kohli, P.; Kumar, R.; Stryhanyuk, H.; Nijenhuis, I.; Lal, R.; Richnow, H. H. Enantiomer and carbon isotope fractionation of  $\alpha$ -hexachlorocyclohexane by *Sphingobium indicum* strain B90A and the corresponding enzymes. *Environ. Sci. Technol.* **2019**, 53, 8715–8724. 573

- 623 (17) Schilling, I. E.; Bopp, C. E.; Lal, R.; Kohler, H. E.; Hofstetter, T.  
624 B. Assessing aerobic biotransformation of hexachlorocyclohexane  
625 isomers by compound-specific isotope analysis. *Environ. Sci. Technol.*  
626 **2019**, *53*, 7419–7431.
- 627 (18) Verma, H.; Bajaj, A.; Kumar, R.; Kaur, J.; Anand, S.; Nayyar,  
628 N.; Puri, A.; Singh, Y.; Khurana, J. P.; Lal, R. Genome Organization of  
629 *Sphingobium indicum* B90A: An Archetypal Hexachlorocyclohexane  
630 (HCH) Degrading Genotype. *Genome Biol. Evol.* **2017**, *9*, 2191–  
631 2197.
- 632 (19) Shrivastava, N.; Macwan, A. S.; Kohler, H. E.; Kumar, A.  
633 Important amino acid residues of hexachlorocyclohexane dehydro-  
634 chlorinases (LinA) for enantioselective transformation of hexachloro-  
635 cyclohexane isomers. *Biodegradation* **2017**, *28*, 171–180.
- 636 (20) Sowińska, A.; Vasquez, L.; Zaczek, S.; Manna, R. N.; Tuñón, I.;  
637 Dybala-Defratyka, A. Seeking the source of catalytic efficiency of  
638 lindane dehydrochlorinase, LinA. *J. Phys. Chem. B* **2020**, *124*, 10353–  
639 10364.
- 640 (21) Manna, R. N.; Zinovjev, K.; Tuñón, I.; Dybala-Defratyka, A.  
641 Dehydrochlorination of hexachlorocyclohexanes catalyzed by the  
642 LinA dehydrohalogenase. A QM/MM study. *J. Phys. Chem. B* **2015**,  
643 *119*, 15100–15109.
- 644 (22) Trantírek, L.; Hynková, K.; Nagata, Y.; Murzin, A.; Ansorgová,  
645 A.; Sklenár, V.; Damborský, J. Reaction mechanism and stereo-  
646 chemistry of gamma-hexachlorocyclohexane dehydrochlorinase LinA.  
647 *J. Biol. Chem.* **2001**, *276*, 7734–7740.
- 648 (23) Tang, X. W.; Zhang, R. M.; Zhang, Q. Z.; Wang, W. X.  
649 Dehydrochlorination mechanism of  $\gamma$ -hexachlorocyclohexane de-  
650 graded by dehydrochlorinase LinA from *Sphingomonas paucimobilis*  
651 UT26. *RSC Adv.* **2016**, *6*, 4183–4192.
- 652 (24) Manna, R. N.; Dybala-Defratyka, A. Insights into the  
653 elimination mechanisms employed for the degradation of different  
654 hexachlorocyclohexane isomers using kinetic isotope effects and  
655 docking studies. *J. Phys. Org. Chem.* **2013**, *26*, 797–804.
- 656 (25) Bashir, S.; Fischer, A.; Nijenhuis, I.; Richnow, H. H.  
657 Enantioselective carbon stable isotope fractionation of hexachloro-  
658 cyclohexane during aerobic biodegradation by *Sphingobium* spp.  
659 *Environ. Sci. Technol.* **2013**, *47*, 11432–11439.
- 660 (26) Schilling, I. E.; Hess, R.; Bolotin, J.; Lal, R.; Hofstetter, T. B.;  
661 Kohler, H. E. Kinetic isotope effects of the enzymatic transformation  
662 of gamma-hexachlorocyclohexane by the lindane dehydrochlorinase  
663 variants LinA1 and LinA2. *Environ. Sci. Technol.* **2019**, *53*, 2353–  
664 2363.
- 665 (27) Kannath, S.; Adamczyk, P.; Wu, L.; Richnow, H. H.; Dybala-  
666 Defratyka, A. Can alkaline hydrolysis of  $\gamma$ -HCH serve as a model  
667 reaction to study its aerobic enzymatic dehydrochlorination by LinA?  
668 *Int. J. Mol. Sci.* **2019**, *20*, 5955.
- 669 (28) Nijenhuis, I.; Renpenning, J.; Kümmel, S.; Richnow, H. H.;  
670 Gehre, M. Recent advances in multi-element compound-specific  
671 stable isotope analysis of organohalides: Achievements, challenges and  
672 prospects for assessing environmental sources and transformation.  
673 *Trends Environ. Anal. Chem.* **2016**, *11*, 1–8.
- 674 (29) Nijenhuis, I.; Richnow, H. H. Stable isotope fractionation  
675 concepts for characterizing biotransformation of organohalides. *Curr.*  
676 *Opin. Biotechnol.* **2016**, *41*, 108–113.
- 677 (30) Torrentó, C.; Ponsin, V.; Lihl, C.; Hofstetter, T. B.; Baran, N.;  
678 Elsner, M.; Hunkeler, D. Triple-Element Compound-Specific Stable  
679 Isotope Analysis (3D-CSIA): Added Value of Cl Isotope Ratios to  
680 Assess Herbicide Degradation. *Environ. Sci. Technol.* **2021**, *55*,  
681 13891–13901.
- 682 (31) Palau, J.; Shouakar-Stash, O.; Hatijah Mortan, S.; Yu, R.; Rosell,  
683 M.; Marco-Urrea, E.; Freedman, D. L.; Aravena, R.; Soler, A.;  
684 Hunkeler, D. Hydrogen Isotope Fractionation during the Biode-  
685 gradation of 1,2-Dichloroethane: Potential for Pathway Identification  
686 Using a Multi-element (C, Cl, and H) Isotope Approach. *Environ. Sci.*  
687 *Technol.* **2017**, *51*, 10526–10535.
- 688 (32) Liu, Y.; Kümmel, S.; Yao, J.; Nijenhuis, I.; Richnow, H.-H. Dual  
689 C–Cl isotope analysis for characterizing the anaerobic transformation  
690 of  $\alpha$ ,  $\beta$ ,  $\gamma$ , and  $\delta$ -hexachlorocyclohexane in contaminated aquifers.  
691 *Water Res.* **2020**, *184*, 116128.
- (33) Badea, S. L.; Vogt, C.; Gehre, M.; Fischer, A.; Danet, A. F.;  
Richnow, H. H. Development of an enantiomer-specific stable carbon  
isotope analysis (ESIA) method for assessing the fate of alpha-  
hexachlorocyclohexane in the environment. *Rapid Commun. Mass*  
*Spectrom.* **2011**, *25*, 1363–1372.
- (34) Wu, L.; Moses, S.; Liu, Y.; Renpenning, J.; Richnow, H. H. A  
concept for studying the transformation reaction of Hexachlorocyclohexanes in food webs using multi-element compound-specific isotope analysis. *Anal. Chim. Acta* **2019**, *1064*, 56–64.
- (35) Horst, A.; Renpenning, J.; Richnow, H.-H.; Gehre, M. Compound specific stable chlorine isotopic analysis of volatile aliphatic compounds using gas chromatography hyphenated with multiple collector inductively coupled plasma mass spectrometry. *Anal. Chem.* **2017**, *89*, 9131–9138.
- (36) Renpenning, J.; Horst, A.; Schmidt, M.; Gehre, M. Online isotope analysis of  $^{37}\text{Cl}/^{35}\text{Cl}$  universally applied for semi-volatile organic compounds using GC-MC-ICPMS. *J. Anal. At. Spectrom.* **2018**, *33*, 314–321.
- (37) Chen, H.; Gao, B.; Wang, S.; Fang, J. Microbial degradation of hexachlorocyclohexane (HCH) pesticides. *Adv. Biodegrad. Biorem. Ind. Waste* **2015**, *10*, 181–210.
- (38) Elsner, M.; Zwank, L.; Hunkeler, D.; Schwarzenbach, R. P. A new concept linking observable stable isotope fractionation to transformation pathways of organic pollutants. *Environ. Sci. Technol.* **2005**, *39*, 6896–6916.